

Unusual Behavior of Ion Transport Mediated by Polyene Antibiotics. Activation Energies for the Exchange of Na⁺ Ions through Liposomal Membranes Studied by ²³Na-NMR Spectroscopy

Atsuomi KIMURA,^a Naohito KUNI,^a and Hideaki FUJIWARA^{*,b}

Faculty of Pharmaceutical Sciences,^a Osaka University, 1–6 Yamadaoka, Suita, Osaka 565, Japan and Faculty of Medicine,^b Osaka University, 2–2 Yamadaoka, Suita, Osaka 565, Japan.

Received September 9, 1996; accepted November 14, 1996

²³Na-NMR spectroscopy has been applied to study the transport of Na⁺ ions across unilamellar vesicle membranes mediated by ionophores. The ionophores used were amphotericin B and nystatin. Also, monensin, lasalocid A and gramicidin D were included for the sake of comparison since the transport processes of these ionophores are well characterized as carrier-, carrier- and channel-types, respectively. The ²³Na-NMR techniques employed were 2D-EXSY (exchange spectroscopy) and the 1D time-course monitoring techniques, and the measurement exchange rates. These techniques were also applied at different temperatures, and the activation parameters were determined for the ionophore-mediated Na⁺ exchange. These activation parameters disclosed an unusual behavior of amphotericin B and nystatin. That is, cation transport through the membrane is decreased on increasing the temperature of measurement, resulting in negative values for the apparent enthalpy of activation. Such unusual behavior is related to the fluidity of the model membrane and to intermolecular interactions in the membrane.

Key words polyene antibiotic; liposomal membrane; cation transport; activation energy; ²³Na-NMR

The antibiotics that belong to the ionophores act on biological membranes and increase the selective permeation of cations.^{1,2)} The ionophores can be divided into two types depending on the mechanism of transport: carrier- and channel-types. Carrier-type ionophores are molecules that bind with ions to form lipid-soluble complexes, and they can diffuse easily in membranes. The channel-type ionophores are believed to transport ions by forming channels across membranes. Clarification of such mechanisms provides a clue to the factors that govern the passive transport of ions through biological membranes and to the generation and transmission of nerve impulses.¹⁾

To date, many studies have been performed to investigate the mechanism of ionophore-mediated cation transport by using liquid, planar lipid bilayer membranes and artificial vesicles.^{2–4)} Among the ionophores, polyether antibiotics such as lasalocid A and monensin have been widely accepted as typical carrier-type ionophores. These ionophores can form complexes with di- as well as monovalent cations and transport the ions through the membrane as a mobile-carrier. Gramicidin, the most accepted channel-type ionophore, is considered to dimerize itself in the membrane and form a channel to transport monovalent cations. Thus, the cation transport mechanism of these ionophores has been well characterized by abundant experimental data.

On the other hand, antifungal polyene antibiotics such as amphotericin B and nystatin (Fig. 1) have been much less studied as ionophores, and the exact mechanism of action for these antibiotics remains unresolved in many respects. The most accepted model of action for these antibiotics is based on the formation of channels with the cooperation of sterol in the biological membrane.⁵⁾ Recently, however, an alternative membrane defect model has been proposed.⁶⁾ In the latter model, amphotericin B forms stable complexes with phospholipids^{7,8)} and

aggregates to form pores in the membrane.⁹⁾ Then, the complexes are organized into a channel form with the aid of sterol molecules. In addition, it has been reported that amphotericin B and nystatin form transport pathways different from those of other channel-type ionophores; that is, they form two types of channels (or pores) depending on whether they are added from one side or both sides of planar membranes or vesicles.^{10,11)} Therefore, it is of interest to study the ion-transport process of these antibiotics and to compare the process with that of the well characterized ionophores of the carrier- or channel-types.

Nuclear magnetic resonance (NMR) enables us to study the dynamics of the transmembrane cation exchange. Here, determining lanthanide shift reagents^{12,13)} which resolve resonances of the intra- and extra-cellular cations has often been utilized as a basic method of investigation. By the use of such shift reagents, dynamic NMR has become applicable, and cation transport processes have been successfully investigated for metal ions such as Li⁺, Na⁺, K⁺ or Ca²⁺. Riddell *et al.* have demonstrated that the ⁷Li magnetization-transfer method can be effectively used to determine the rate constants of an ionophore-mediated transmembrane exchange of Li⁺.¹⁴⁾ More recently, Shungu and co-workers successfully used the ²³Na inversion-transfer method to study the transport of ion-carrier monensin^{15,16)} using unilamellar phospholipid membrane vesicles. These NMR techniques can be applied *in situ*. The techniques, however, have not been applied widely because the range of exchange rate is so widely distributed that any one special technique is insufficient to cover the wide range of rates exhibited by different ionophores.

In the present study, different NMR techniques were utilized together, and the rate constants of Na⁺ transmembrane exchange were measured under the influence of polyene antibiotics. Furthermore, activation parameters

* To whom correspondence should be addressed.

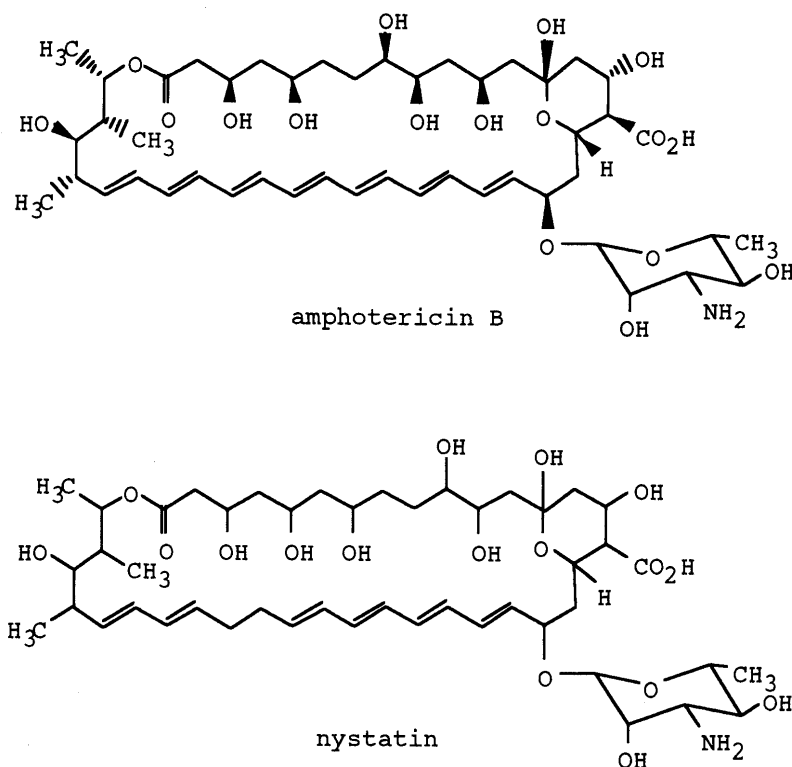


Fig. 1. Chemical Structures of Amphotericin B and Nystatin

were determined for the exchange process and compared with the results of monensin, lasalocid A and gramicidin D.

Experimental

Materials Cholesterol was purchased from Wako Pure Chemical Industry, Ltd. and recrystallized from methanol. The egg lecithin (Merck Chemical Co.) was ascertained to give only a single spot on a Silicagel 60 plate in thin-layer chromatography. Benzyl alcohol (Wako Pure Chemical Ind., Ltd.) was distilled twice. Other chemicals of analytical grade were used without further purification: monensin sodium salt, amphotericin B, nystatin, sodium tripolyphosphate and dysprosium chloride (Wako Pure Chemical Ind., Ltd.); lasalocid A and gramicidin D (Sigma Chemical Co.).

Preparation of Na⁺-Entrapped Large Unilamellar Vesicles and Samples for NMR Measurement Na⁺ ions were entrapped in large unilamellar vesicles (LUV) by the reverse-phase evaporation method developed by Szoka and Papahadjopoulos.¹⁷⁾ Egg yolk phosphatidylcholine (100 mg) was dissolved in 6 ml of diethyl ether distilled immediately prior to use. Then, a 2 ml solution of 100 mM NaCl buffered at pH 7.6 (10 mM phosphate buffer) was added to the lipid/ether mixture. The resulting two-phase suspension was sonicated at 0 °C in a bath-type sonicator for 5–10 min to form a homogeneous emulsion. Finally, the phase of ethyl ether was slowly removed by rotary evaporation at room temperature, leaving a translucent aqueous suspension of vesicles. LUV, containing 20% cholesterol by weight, was prepared if necessary (to measure Na⁺ exchange rates mediated by the polyene antibiotics). The size homogeneity of the vesicles was checked by the dynamic light scattering using a PLS-700 spectrometer (Otsuka Electron Co.), and the average diameter was obtained at 203 nm. For ²³Na-NMR 1D time-course measurement (see Results and Discussion) the NaCl-containing LUV was further dialyzed twice against 2 l of 100 mM KCl and 10 mM phosphate buffer for 6–10 h to replace external Na⁺ with K⁺, while the dialysis was unnecessary for ²³Na 2D-EXSY (exchange spectroscopy) measurement.

An 8 mM solution of bis(tripolyphosphate) dysprosium ion, Dy(PPP)₂⁷⁻ · 7Na⁺, and shift reagent was prepared according to the method described by Gupta *et al.*¹²⁾ For 1D time-course measurement, an alternative solution of Dy(PPP)₂⁷⁻ · 7K⁺ was prepared.¹⁸⁾ An NMR sample was made by mixing 0.2 ml of deuterium oxide, 0.9 ml of Dy(PPP)₂⁷⁻ and

0.9 ml of the vesicle solution.

Monensin, lasalocid A and gramicidin D were dissolved in methanol and the polyene antibiotics, nystatin and amphotericin B, were dissolved in dimethyl sulfoxide (DMSO). These solutions were volumetrically added to an NMR sample, using a microsyringe, on the measurement of exchange rate constants, so that the sample included 0.2 mM of the ionophore except amphotericin B (0.2 μM). The measurement of the Na⁺ exchange rate constant was repeated more than twice using different batches of the sample.

NMR Measurement ²³Na-NMR spectra were recorded at 52.9 MHz on a Varian VXR-200 spectrometer. The condition of 1D ²³Na-NMR measurement was typically: 90° pulse width = 11.0 μs; pulse cycle = 0.1 s; accumulation times = 64–256 scans.

2D-EXSY ²³Na-NMR spectra were measured using the NOESY pulse sequence, PD-90°-t₁-90°-t_m-90°-t₂, where t_m is the mixing time during which spin transfer occurs as a result of the exchange process, causing cross peaks to appear between diagonal peaks in the 2D spectral map. The mixing time, t_m, was typically set to 10–20 ms.¹⁵⁾ The measurement was made with States-Haberhorn data collection.¹⁹⁾ Data sets with F₁ and F₂ dimensions of 256 and 1024, respectively, were collected. The data were multiplied by a Gaussian window function in both the F₁ and F₂ dimensions.

Results and Discussion

Measurement of Na⁺ Exchange Rates by Time-Course Analysis of ²³Na 1D-NMR Spectra Figure 2 illustrates the ²³Na-NMR spectrum of a dispersion of LUV prepared from egg lecithin: in the NMR tube, 100 mM NaCl was included inside the vesicles and the aqueous phase outside the vesicles contained 100 mM KCl, <0.5 mM NaCl and 3.6 mM Dy(PPP)₂⁷⁻. Figure 2a shows the spectrum observed without ionophore, which indicates clearly that the resonances of intra- and extravesicle Na⁺ ions were resolved by the addition of Dy(PPP)₂⁷⁻ shift reagent. The larger and smaller peaks were assigned to Na⁺ inside and outside the vesicles, respectively, since Dy(PPP)₂⁷⁻ is known to cause an upfield shift of ²³Na⁺ resonance.¹³⁾ The very small peak of ²³Na⁺ outside the vesicles in Fig.

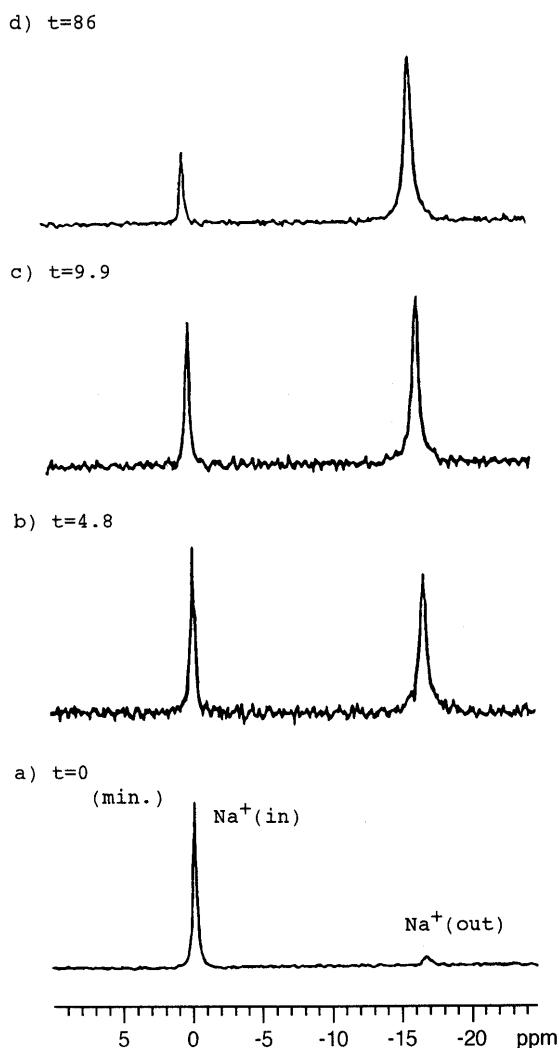


Fig. 2. ²³Na-NMR Spectra of Sodium Ions Inside and Outside Vesicles at 25°C

a) The spectrum was obtained in the absence of nystatin. In the sample, the concentrations were: ca. 27 mM LUV; 100 mM NaCl inside the vesicles; 100 mM KCl and 3.6 mM Dy(PPP)₂²⁻ outside the vesicles. b—d) Spectra are labeled with the minutes elapsed after nystatin (0.2 mM) was added to the sample.

2 supports a successful dialysis, when compared with a previously reported result.²⁰⁾ This sample was subjected to the measurement of transmembrane exchange rates.

Immediately after the observation of Fig. 2a, nystatin dissolved in DMSO was added so that the sample included 0.2 mM of the ionophore. Figure 2b—d illustrate the time dependence of the leakage of internal Na⁺ ions induced by nystatin. It is seen that the outer peak increased in area at the expense of the inner peak, indicating the induced efflux of Na⁺.

To analyze the time course of efflux of Na⁺ ions, Eq. 2 is derived from the reversible pseudo first-order reaction rate law (Eq. 1),



$$-\frac{d[\text{Na}_{in}^+]}{dt} = k_1[\text{Na}_{in}^+] - k_2[\text{Na}_{out}^+] \quad (2)$$

where k_1 and k_2 are the pseudo first-order reaction rate constants of efflux and influx of Na⁺ ions, respectively.

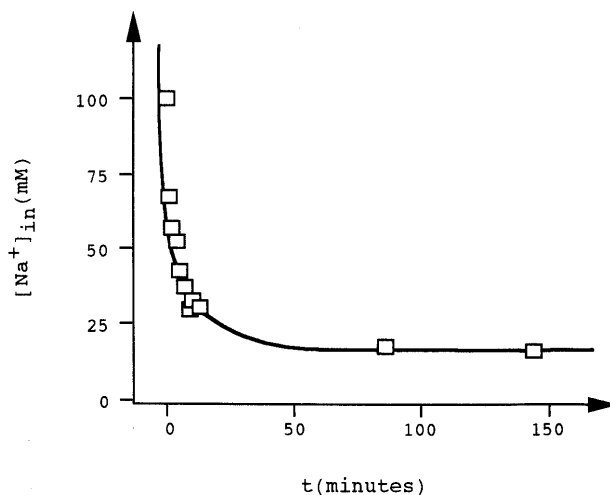


Fig. 3. The Time Dependence of the Concentration of Na⁺ Inside Vesicles Obtained from Fig. 2

The result of non-linear least square fitting is also included. The best fit solution was obtained at $k_1 = 4.40 \times 10^{-3} \text{ s}^{-1}$ and $k_2 = 6.12 \times 10^{-3} \text{ s}^{-1}$.

An integrated law (Eq. 4) can be obtained from Eq. 2 under the condition of Eq. 3:

$$V_{in}[\text{Na}_{in}^+] + V_{out}[\text{Na}_{out}^+] = C \quad (\text{constant}) \quad (3)$$

$$\int_{[\text{Na}_{in}^+]_{t=0}}^{[\text{Na}_{in}^+]_{t=t}} \frac{d[\text{Na}_{in}^+]}{a[\text{Na}_{in}^+] + b} = \int_{t=0}^{t=t} a dt \quad (4)$$

where V_{in} and V_{out} are the total inner and outer volumes of LUV vesicles, respectively, and $a = k_1 + k_2 \times V_{in}/V_{out}$ and $b = -k_2 \times C/V_{out}$. Then Eq. 5 is obtained by solving Eq. 4.

$$[\text{Na}_{in}^+]_{t=t} = \frac{C/V_{in} + b(1 - e^{at})/a}{e^{at}} \quad (5)$$

Equation 5 represents the rate law of the efflux of Na⁺ ions. Therefore, the experimental results of Fig. 3 can be analyzed by Eq. 5, leading to the determination of the pseudo first-order exchange rate constants k_1 and k_2 .

From Fig. 2, the concentration of inner Na⁺ ions was plotted against time (Fig. 3). The value of V_{in} and V_{out} necessary to calculate the concentration was evaluated by multiplying the total sample volume by the relative inside and outside peak area (0.15 and 0.85, respectively) after the Na⁺ exchange reached sufficient equilibrium (Fig. 2d). Then, the Na⁺ concentration at time zero (Fig. 2a) was converted to include 100 mM of Na⁺. Figure 3 also shows the result of a non-linear least-square analysis using Eq. 5. For this analysis a SALS program was adopted.²¹⁾

Table 1 shows the rate constants (k_1) for the exchange of Na⁺ ions at different temperatures induced by nystatin and amphotericin B. The concentration of amphotericin B (0.2 μM) had to be a thousandth part of nystatin (0.2 mM), since it sufficiently induced a moderate range of exchange rate for 1D time-course measurement. However, the order of these rate constants was about a hundred times larger than that of the un-assisted limiting diffusion rate at 25°C, $1.11(\pm 0.20) \times 10^{-6} \text{ s}^{-1}$, measured by the same method, and the reproducibility was sufficiently good, supporting the validity of our method.

The rate constants observed above imply a passive transport of Na⁺ at the expense of K⁺ mediated by the

Table 1. Temperature Dependence of Na⁺ Exchange Rate Constants ($\times 10^{-4} \text{ s}^{-1}$) Measured by 1D Time-Course Analysis

Ionophore	T (K)					
	298	303	308	313	318	328
Nystatin	49.8 (2.0)		7.4 (2.1)		2.7 (0.5)	1.4 (0.1)
Amphotericin B	22.8 (2.5)	7.9 (0.6)	5.9 (0.3)	3.1 (0.3)		
Amphotericin B + benzyl alc.	2.1 (0.3)		2.8 (0.3)	4.4 (0.4)		

Standard deviations are given in the parentheses.

Table 2. Temperature Dependence of Na⁺ Transmembrane Exchange Rate Constants (s^{-1}) Measured by 2D-EXSY

Ionophore	T (K)						
	298	303	308	313	323	333	343
Monensin	16.0 (2.3)	18.9 (2.3)		38.9 (3.6)	42.8 (3.4)	139 (11.0)	
Lasalocid A			1.1 (0.3)	1.4 (0.2)	1.8 (0.2)	2.6 (0.3)	5.0 (0.4)
Gramicidin D	7.0 (0.6)	14.3 (1.9)		17.4 (0.9)	26.6 (1.5)	42.1 (2.3)	

Standard deviations are given in the parentheses.

ionophores. In this case, both Na⁺ and K⁺ ions are transported against the gradient in the concentration of each ion. Here, the exchange of Na⁺ ions is considered to be rate-determining since the polyene antibiotic induces K⁺ transport much larger than Na⁺.⁵⁾ Therefore, the rate constants observed here are interpreted to denote the transmembrane exchange rates of Na⁺ ions.

2D-EXSY ²³Na-NMR Measurement Dynamic NMR methods are suitable for monitoring exchange rates which are larger than the longitudinal relaxation rate (T_1^{-1}).¹⁶⁾ The exchange rate at equilibrium condition can be obtained by this method of analysis. Among several versions of these dynamic NMR methods, two dimensional NMR exchange spectroscopy (2D-EXSY) has recently been gaining popularity as a powerful tool for kinetic studies.^{22,23)} So, we have tried to apply this technique to the cation transport in our vesicle system.

Figure 4 shows the 2D-EXSY spectrum measured to analyze the transmembrane Na⁺ exchange promoted by monensin. The parameters of the 2D-EXSY measurement were set according to the procedure proposed by Jeener *et al.*²⁴⁾ The cross peaks between the diagonal peaks clearly indicate the presence of an exchange process $^{23}\text{Na}_{\text{in}}^+ \leftrightarrow ^{23}\text{Na}_{\text{out}}^+$. Volume intensities of the cross- and diagonal peaks were measured in Fig. 4, and the exchange rates could be evaluated quantitatively by Abel's procedure.²³⁾ Table 2 shows the rate constants of Na⁺ exchange mediated by monensin, lasalocid A and gramicidin D at different temperatures. The order of these values was comparable to that of the T_1^{-1} of inside and outside the vesicles, 21.1 s⁻¹ and 59.1 s⁻¹ (25 °C), respectively. The rate constant of this range was obtained successfully, as seen in Table 2, since the range is well suited for the 2D-EXSY experiment,²²⁾ while it would have been too fast for measurement by 1D time-course analysis.

It should be noted that the rate constant obtained by the 2D-EXSY technique is the one in the equilibrium state of concentration, which is not necessarily equivalent to the result obtained from the 1D time-course analysis (vide supra) which is made under a gradient of the ion concen-

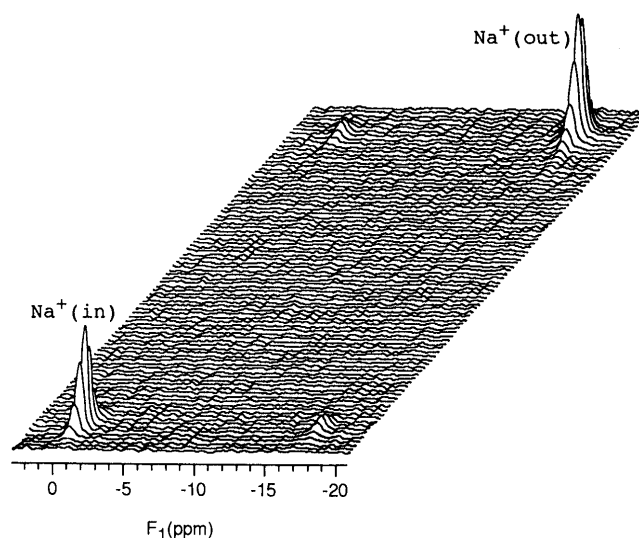


Fig. 4. ²³Na 2D-EXSY Spectrum of a LUV Suspension at 25°C in the Presence of Monensin

The sample contains ca. 27 mM LUV, 100 mM NaCl, 0.2 mM monensin and 3.6 mM Dy(PPP)₂⁷⁻ outside the vesicles. The mixing time, t_m , was 11 ms.

tration. Therefore, the Na⁺ exchange rates derived from the 2D-EXSY method may not be comparable with those of the 1D time-course analysis. However, the cation transport rates of various ionophores cover a wide range of time scale, and such a difference in measuring methods may be inevitable. The limited range of exchange rate can be measured by a duplicate method and it has been reported that the difference between these methods does not pose a critical problem.²⁵⁾ In the following, the discussion is extended to the activation parameters of cation transport.

Results from the Temperature-Dependence Experiments

The activation parameters were obtained for the transport process from analysis of the temperature dependence of the rate constant according to the Eyring absolute rate theory¹⁶⁾: the Gibbs free energy (ΔG^\ddagger), the enthalpy (ΔH^\ddagger), and the entropy (ΔS^\ddagger) of activation were obtained from Eyring's formulation of the temperature dependence

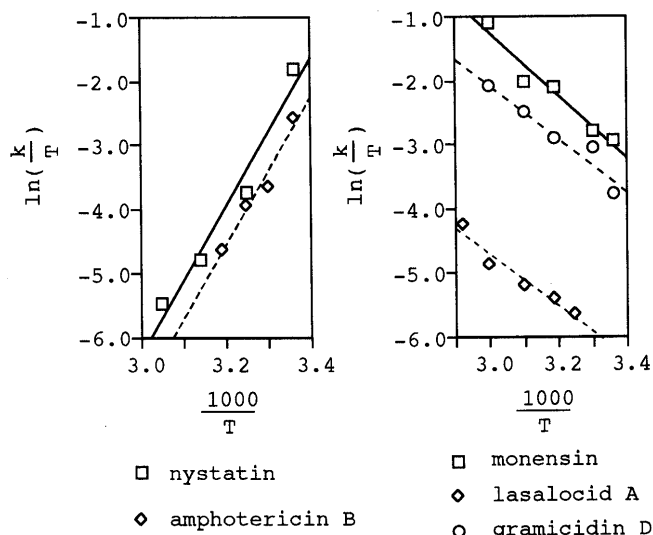


Fig. 5. Eyring Plots Showing the Temperature Dependencies of the Na⁺ Transmembrane Exchange Rate Constants

Table 3. Thermodynamic Properties of Na⁺ Ion Transport across the Liposome Bimolecular Membrane Mediated by Several Ionophores

Ionophore	ΔH^\ddagger (kJ mol ⁻¹)	$T\Delta S^\ddagger$ (kJ mol ^{-1 a)})	ΔG^\ddagger (kJ mol ⁻¹)
Monensin	40 ± 9	-26 ± 9	66 ± 13
Lasalocid A	33 ± 5	-41 ± 4	74 ± 6
Gramicidin D	28 ± 4	-39 ± 4	67 ± 6
Nystatin	-98 ± 3	-185 ± 27	87 ± 6
Amphotericin B	-94 ± 15	-183 ± 15	89 ± 21
Amphotericin B + benzyl alc.	33 ± 8	-61 ± 8	94 ± 11

a) 298.15 K.

of the rate constant. The logarithmic form of this equation is written as:

$$\ln\left(\frac{k}{T}\right) = -\frac{\Delta G^\ddagger}{RT} + \ln\left(\frac{k}{h}\right) = -\frac{\Delta H^\ddagger}{RT} + \frac{\Delta S^\ddagger}{R} + \ln\left(\frac{k}{h}\right) \quad (6)$$

where k is the Boltzmann constant, and h is Planck's constant. ΔG^\ddagger was calculated using $\Delta G^\ddagger = \Delta H^\ddagger - T\Delta S^\ddagger$.

Figure 5 shows the Eyring plot obtained from data listed in Tables 1 and 2. The correlation coefficients of the plot analyzed by Eq. 6 were 0.97 (monensin, lasalocid A and gramicidin D) and 0.98 (nystatin and amphotericin B). The derived activation parameters are listed in Table 3. The activation enthalpy values of monensin, lasalocid A and gramicidin D show good agreement with reported values obtained using artificial membranes, as mentioned in the following discussion.^{16,26} However, the activation enthalpy of Na⁺ transport is clearly shown to be unusual when mediated by the polyene antibiotics, nystatin and amphotericin B. That is to say, negative temperature dependencies are obtained for the exchange processes for nystatin and amphotericin B. To the authors' knowledge, such observation has not been reported until now.

In order to interpret the meaning of the activation parameters of the monensin- and gramicidin-mediated cation transport, a hypothetical energy barrier model has

been proposed.^{2,16} The model is composed of rate processes which give rise to energy barriers in which a cation is expected to be encountered in moving from one side of the membrane to the other. The rate mechanism is separated into three processes: (A) binding of the cation to the ionophore at the membrane-solution interface (this step is characterized by the association rate constant); (B) migration or diffusion of the cation across the membrane (this is characterized by the diffusion rate constant); (C) dissociation of the cation at the opposite side of the membrane (this is characterized by the dissociation rate constant). Although there are three individual rate constants to be determined, the NMR-based method has yielded only one rate constant for the total process. That is, the NMR-derived rate constant contains contributions from all three individual rate processes. However, when one of these three steps occurs at a rate much slower than the other two, that is when the major contribution will surely come from this "rate determining" process.

Shung *et al.* have determined the activation parameters of monensin-mediated Na⁺ transport in the LUV membrane, and found good agreement between the ΔH^\ddagger values of the transport (41.9 kJ/mol) and the complexation of monensin with Na⁺ measured in methanol (43.2 kJ/mol) in which the dissociation reaction is the rate determining process.¹⁶ From these results, they concluded that the rate determining process of the transport is the dissociation process (C). As seen in Table 3, these reported ΔH^\ddagger values correspond well to the value obtained in the present study. As for the Na⁺ transport of the gramicidin-channel, the rate determining process of the transport is also considered to be the dissociation process (C).²⁷ Moreover, the ΔH^\ddagger value of the dissociation process has been reported to be 28 kJ/mol from the analysis of Na⁺ interaction with gramicidin channels incorporated into the lysolecithin micelle system,²⁷ which also corresponds well to our result. The agreement between these reported values and our results indicates that the ΔH^\ddagger values obtained in the present study characterize the same mechanism of Na⁺ transport in the case of monensin, lasalocid A and gramicidin D. That is, the rate-determining process is the dissociation process (C) in the above mentioned model.

The ΔH^\ddagger values of amphotericin B and nystatin clearly indicate that the transport mechanism of these polyene antibiotics is different from that of the other carrier- and channel-type ionophores (Table 3). This is understandable from the idea that the polyene antibiotic molecules aggregate to form a channel (or pore) in cooperation with sterol or lipid molecules contained in the membrane, as mentioned in the Introduction. It has been soundly determined that the aggregation of amphotericin B in the artificial membrane is prevented by raising the temperature.⁸ From these facts, it is conceivable that the cation transport mediated by polyene antibiotics is governed by the molecular interactions between polyene antibiotics and the membrane-composing molecules. According to this idea, the factor that affords the negative values for the enthalpy of amphotericin B and nystatin is the frequency of channel-formation as well as the probability of a channel-opening state: the frequency and

probability decrease as the temperature is increased because of the enhanced Brownian motion of the ionophore molecules as well as the enhanced fluidity of the membrane medium at elevated temperatures.

To confirm this hypothesis, benzyl alcohol, one of the anesthetics that increases the fluidity of membranes,²⁸⁾ was added to the sample containing amphotericin B at an equimolar ratio (benzyl alcohol/amphotericin B = 0.2 μM /0.2 μM). Under this condition, benzyl alcohol was confirmed not to affect Na^+ efflux by itself. Then, the activation enthalpy of Na^+ exchange promoted by amphotericin B changed its sign, appearing as a positive value (Table 3). This observation also supports the dependence of Na^+ transport upon membrane fluidity in polyene antibiotic channels.

Recently, a membrane defect model has been proposed for the action of these antibiotics in place of the traditionally accepted model⁶⁾ based on the formation of channels with sterols involved in the biological membranes. In this model, amphotericin B interacts with the membrane phospholipids, and sterols help these complexes to be organized into channels. These characteristic features of biological membranes will surely affect the activation parameters of the ion transport, and our findings for the unusual behavior of polyene antibiotics is related to membrane models as well as to intermolecular interactions in membranes that affect ion-channel formation.

References

- 1) Pullman A., *Chem. Rev.*, **91**, 793—812 (1991).
- 2) Lauger P., *Angew. Chem. Int. Ed. Engl.*, **24**, 905—923 (1985).
- 3) Ashton R., Steinrauf L. K., *J. Mol. Biol.*, **49**, 547—556 (1970).
- 4) Degani H., *Biochim. Biophys. Acta*, **509**, 364—369 (1978).
- 5) Kruijff B. D., Gerritsen W. J., Oerlemans A., Demel R. A., Van L. L. M., *Biochim. Biophys. Acta*, **339**, 30—43 (1974).
- 6) Hartsel S. C., Benz S. K., Peterson R. P., Whyte B. S., *Biochemistry*, **30**, 77—82 (1991).
- 7) Balakrishnan A. R., Easwaren K. R. K., *Biochim. Biophys. Acta*, **1148**, 269—277 (1993).
- 8) Balakrishnan A. R., Easwaren K. R. K., *Biochemistry*, **32**, 4139—4144 (1993).
- 9) Bolard J., Legrand P., Heitz F., Cybulska B., *Biochemistry*, **30**, 5707—5715 (1991).
- 10) Kleinberg M. E., Finkelstein A., *J. Membrane Biol.*, **80**, 257—269 (1984).
- 11) Hartsel S. C., Perkins W. R., McGarvey G. J., Cafiso D. S., *Biochemistry*, **27**, 2656—2660 (1988).
- 12) Gupta R. K., Gupta P., *J. Magn. Reson.*, **47**, 344—350 (1982).
- 13) Gupta R. K., Gupta P., *Ann. Rev. Biophys. Bioeng.*, **13**, 221—246 (1982).
- 14) Riddel F. G., Arumugam S., Cox B. G., *J. Chem. Soc. Chem. Commun.*, **1987**, 1890—1891.
- 15) Shungu D. C., Briggs R. W., *J. Magn. Reson.*, **77**, 491—503 (1988).
- 16) Shungu D. C., Buster D. C., Briggs R. W., *J. Magn. Reson.*, **89**, 102—122 (1990).
- 17) Szoka F., Olson F., Heath T., Vail W., Wayhew E., Papahadjopoulos D., *Biochim. Biophys. Acta*, **601**, 559—571 (1980).
- 18) Chu S. C., Pike M. M., Fossel E. T., Smith T. W., Balschi J. A., Springer C. S., *J. Magn. Reson.*, **56**, 33—47 (1984).
- 19) States D. J., Haberkorn R. A., Ruben D. J., *J. Magn. Reson.*, **48**, 286—292 (1982).
- 20) Pike M. M., Simon S. R., Balschi J. A., Springer C. S., *Proc. Natl. Acad. Sci. U.S.A.*, **79**, 810—814 (1982).
- 21) Nakagawa T., Oyanagi Y., "Program System for Statistical Analysis with Least-Squares Fitting, SALS (version 2). Users' Manual," Univ. of Tokyo Computer Centre, Tokyo, 1979.
- 22) Perrin C. L., Dwyer T. J., *Chem. Rev.*, **90**, 935—967 (1990).
- 23) Abel E. W., Coston T. P. J., Orrell K. G., Sik V., Stephenson D., *J. Magn. Reson.*, **70**, 34—53 (1986).
- 24) Jeener J., Meier B. H., Bacmann P., Ernst R. R., *J. Chem. Phys.*, **71**, 4546—4553 (1979).
- 25) Orrell K. G., Stephenson D., Rault T., *Magn. Reson. Chem.*, **27**, 368—376 (1989).
- 26) Urry D. W., Venkatachalam C. M., Spisni A., Lauger P., Khaled M. A., *Proc. Natl. Acad. Sci. U.S.A.*, **77**, 2028—2032 (1980).
- 27) Urry D. W., Spisni A., Khaled M. A., *Biochem. Biophys. Res. Commun.*, **88**, 940—949 (1979).
- 28) Gupta S. P., *Chem. Rev.*, **91**, 1109—1119 (1991).